Ku70 Is Required for DNA Repair but Not for T Cell Antigen Receptor Gene Recombination In Vivo

By Honghai Ouyang,* Andre Nussenzweig,* Akihiro Kurimasa,‡ Vera da Costa Soares,* Xiaoling Li,* Carlos Cordon-Cardo,* Wen-hui Li,§ Nge Cheong,§ Michel Nussenzweig,‖ George Iliakis,§ David J. Chen,‡ and Gloria C. Li*

*From the *Department of Medical Physics and Department of Radiation Oncology, Memorial Sloan-Kettering Cancer Center, New York, 10021; ‡Los Alamos National Laboratory, Los Alamos, New Mexico 87545; §Thomas Jefferson University, Philadelphia, Pennsylvania 19107; ‖Rockefeller University, New York, 10021*

Summary

Ku is a complex of two proteins, Ku70 and Ku80, and functions as a heterodimer to bind DNA double-strand breaks (DSB) and activate DNA-dependent protein kinase. The role of the Ku70 subunit in DNA DSB repair, hypersensitivity to ionizing radiation, and V(D)J recombination was examined in mice that lack Ku70 (*Ku70*$^{-/-}$). Like *Ku80*$^{-/-}$ mice, *Ku70*$^{-/-}$ mice showed a profound deficiency in DNA DSB repair and were proportional dwarfs. Surprisingly, in contrast to Ku80$^{-/-}$ mice in which both T and B lymphocyte development were arrested at an early stage, lack of Ku70 was compatible with T cell receptor gene recombination and the development of mature CD4^{+}CD8^{-} and CD4^{-}CD8^{+} T cells. Our data shows, for the first time, that Ku70 plays an essential role in DNA DSB repair, but is not required for TCR V(D)J recombination. These results suggest that distinct but overlapping repair pathways may mediate DNA DSB repair and V(D)J recombination.

Two distinct processes involving DNA double-strand breaks (DSB)[1] have been identified in mammalian cells: the repair of DNA damage induced by ionizing radiation and V(D)J recombination during T and B cell development. So far, all mammalian cell mutants defective in DNA DSB repair share the common phenotype of hypersensitivity to radiation and impaired ability to undergo V(D)J recombination (1–6). Cell fusion studies using DSB repair mutants of human–rodent somatic hybrids have defined four ionizing radiation (IR) complementation groups: IR4, IR5, IR6, and IR7. Genetic and biochemical analyses have revealed that cells of IR5 (e.g., xrs-6) and IR7 (e.g., *scid*) are defective in components of the DNA-dependent protein kinase (DNA-PK) (2, 7–9). DNA-PK is a serine/threonine kinase comprised of a large catalytic subunit and a DNA-targeting component termed Ku, which itself is a heterodimer of a 70- (Ku70) and a 86-(Ku80) kD polypeptide (10–12). Recently, the DNA-PK catalytic subunit has been shown to be the gene responsible for the murine *scid* defect (13–15), and *Ku80* has been identified to be *XRCC5* (16–18), the x-ray repair cross-complementing gene for IR5. *Ku80* knockout mice were found to exhibit *scid*, defective processing of V(D)J recombination intermediates, and growth retardation (19, 20).

Although *Ku70* has been designated as *XRCC6* (7, 8) and is an important component of the DNA-PK complex, the function of Ku70 in vivo is hitherto unknown. To define the role of Ku70 in DNA repair and V(D)J recombination, we targeted the *Ku70* gene in mice. *Ku70* homozygotes exhibit proportional dwarfism, a phenotype of *Ku80*$^{-/-}$, but not of *scid* mice. Absence of Ku70 confers hypersensitivity to ionizing radiation and deficiency in DNA DSB repair, which are characteristics of both *Ku80*$^{-/-}$ and *scid* mice. Surprisingly, in contrast to *Ku80*$^{-/-}$ and *scid* mice in which both T and B lymphocyte development are arrested at early stage, lack of Ku70 is compatible with T cell receptor gene recombination and the development of mature CD4^{+}CD8^{-} and CD4^{-}CD8^{+} T cells. Our data, for the first time, provide direct evidence supporting that Ku70 plays an essential role in DNA DSB repair, but is not required for TCR gene recombination. These results suggest that distinct but overlapping repair pathways may mediate DSB repair and V(D)J rejoining; furthermore, it suggests the presence of a Ku70-independent rescue pathway in

[1]*Abbreviations used in this paper:* AFIGE, asymmetric field inversion gel electrophoresis; CFU-GM, granulocyte/macrophage CFUs; DNA-PK, DNA-dependent protein kinase; DSB, double-strand break, ES, embryonic stem; Gy, Gray; IR, ionizing radiation; IVS, intervening sequence; SP, single-positive.

J. Exp. Med. © The Rockefeller University Press • 0022-1007/97/09/921/09 $2.00
Volume 186, Number 6, September 15, 1997 921–929
http://www.jem.org

TCR V(D)J recombination. The distinct phenotype of *Ku70*$^{-/-}$ mice should make them valuable tools for unraveling the mechanism(s) of DNA repair and recombination.

Materials and Methods

Target Disruption of Ku70 and Generation of Ku70$^{-/-}$ *Mice.* Mouse genomic *Ku70* gene was isolated from a sCos-I cosmid library constructed from a mouse strain 129 embryonic stem (ES) cell lines (21). The replacement vector was constructed using a 1.5 kb 5′-fragment that contains the promoter locus with four GC boxes and exon 1, and an 8-kb EcoRV–EcoRI fragment extending from intron 2 to intron 5 as indicated in Fig. 1 *A*. Homologous replacement results in a deletion of 336-bp exon 2 including the translational initiation codon.

The targeting vector was linearized with NotI and transfected into CJ7 ES cells by electroporation using a gene pulser (Bio Rad Labs., Hercules, CA). 300 ES cell clones were screened, and five clones carrying the mutation in *Ku70* were identified by Southern blotting. Positive ES clones were injected separately into C57BL/6 blastocysts to generate chimeric mice. One clone was successfully transmitted through the germline after chimeras were crossed with C57BL/6 females. Homozygous *Ku70*$^{-/-}$ mice were generated by crossing *Ku70*$^{+/-}$ heterozygotes.

The genotype of the mice was first determined by tail PCR analysis which distinguishes endogenous from the targeted *Ku70* allele, and subsequently confirmed by Southern blot analysis. The PCR reaction contained 1 μg genomic DNA; 0.6 μM (each) of primers HO-2: GGGCCAGCTCATTCCTCCACTCATG, HO-3: CCTACAGTGTACCCGGACCTATGCC, and HO-4: CGGAACAGGACTGGTGGTTGAGCC; 0.2 mM (each) deoxynucleoside triphosphate; 1.5 mM $MgCl_2$, and 2.5 U of Taq polymerase. Cycling conditions were 94°C for 1 min, 64°C for 1 min, 72°C for 1 min (30 cycles), followed by an extension at 72°C for 10 min. Primers HO-2 and HO-4 give a product of the targeted allele that is ~380 bp; primers HO-3 and HO-4 yield a wild-type product of 407 bp.

Western Blot Analysis and Gel Mobility Shift Assay. To confirm that the disruption of *Ku70* produces a null mutation, Ku70 protein expression was measured by Western blotting using polyclonal antisera against intact mouse Ku70. The lack of Ku70 was also verified by a Ku–DNA-end–binding assay (gel mobility shift analysis). Cell extracts were prepared and gel mobility shift assays were performed as described (22). Equal amounts of cellular protein (50 μg) from *Ku70*$^{+/+}$ (wild type), *Ku70*$^{+/-}$, and *Ku70*$^{-/-}$ mouse embryo fibroblasts were incubated with a ^{32}P-labeled double-stranded oligonucleotide, 5′-GGGCCAAGAATCTTCCAGCAGTTTCGGG-3′. The protein-bound and free oligonucleotides were electrophoretically separated on a 4.5% native polyacrylamide gel. Gel slabs are dried and autoradiographed with X-Omat film (Kodak, Rochester, NY).

Immunohistochemistry. To determine the pathological changes, histological sections of various organs of *Ku70*$^{-/-}$, *Ku80*$^{-/-}$, and wild-type littermate mice were prepared and examined as previously described (23). Lymph nodes, spleens, and thymuses from 4–5-wk-old mice were fixed in 10% buffered formalin and embedded in paraffin, or embedded in (optimal cutting temperature) compound (Sakura Finetek, USA, Incorp., Torrance, CA) and frozen in liquid nitrogen at −70°C. Sections (5 μm) were stained with hematoxylin and eosin, and representative samples were selected for immunohistochemical analysis. Immunophenotyping was performed using an avidin-biotin immunoperoxidase technique (24). Primary antibodies included anti-CD3 (purified rabbit serum, 1:1,000; Dako Corp., Carpinteria, CA), anti-B220 (rat monoclonal, 1:1,000; PharMingen, San Diego, CA), and anti-CD19 (rat monoclonal, 1:1,000; PharMingen), and were incubated overnight at 4°C. Samples were subsequently incubated with biotinylated secondary antibodies (Vector Labs., Burlingame, CA) for 30 min (goat anti–rabbit, 1:100; rabbit anti–rat, 1:100), and then with avidin-biotin peroxidase (1:25 dilution; Vector Labs.) for 30 min. Diaminobenzadine was used as the chromogen and hematoxylin as the counter stain. Wild-type lymphoid organs including thymus, spleen, and lymph nodes from different mice were used for titration of the antibodies and positive controls. Anti-CD3 and anti-CD19 antibodies were tested in both frozen and paraffin sections of wild-type lymphoid organs and showed the expected specific patterns of staining (data not shown). For negative controls, primary antibodies were substituted with class-matched but unrelated antibodies at the same final working dilutions.

Cell Preparation and Flow Cytometric Analysis. For flow cytometry, single cell suspensions from lymphoid organs of 4–6-wk-old mutant and littermate control mice were prepared for staining as described previously (19) and analyzed on a FACScan® with Cell Quest software (Becton Dickinson, San Jose, CA). Cells were stained with combinations of PE-labeled anti-CD4 and FITC-labeled anti-CD8, or PE-labeled anti-B220 and FITC-labeled anti-CD43, or FITC–anti-IgM and PE–anti-B220 (PharMingen), as needed. Bone marrow cells were harvested from femurs by syringe lavage, and cells from thymus and spleen were prepared by homogenization. Cells were collected and washed in PBS plus 5% FCS and counted using a hemacytometer. Samples from individual mice were analyzed separately. Dead cells were gated out by forward and side scatter properties. Experiments were performed at least three times and yielded consistent results.

DNA Preparation and Analysis of V(D)J Recombination Products. To determine whether a null mutation in *Ku70* affects the recombination of antigen-receptor genes in T and B lymphocytes in vivo, we measured the immunoglobulin and T cell antigen receptor (TCR) rearrangements by PCR. DNA from bone marrow was amplified with primers specific to immunoglobulin D-J_H and V-DJ_H rearrangements, and DNA from thymus was amplified with primers that detect V-DJ_β and D_δ-J_δ rearrangement (20, 25–28).

Oligonucleotides for probes and PCR primers specific to TCR V_β-J_β rearrangements and immunoglobulin D-J_H and V-DJ_H rearrangements are as follows. For TCR-β V_β8-J_β2 rearrangements (28): V_β8.1:5′-GAGGAAAGGTGACATTGAGC-3′, J_β2.6: 5′-GCCTGGTGCCGGGACCGAAGTA-3′, V_β8 probe: 5′-GGGCTGAGGCTGATCCATTA-3′. For $D_{\delta 2}$-$J_{\delta 1}$ rearrangements (20, 27): DR6: 5′-TGGCTTGACATGCAGAAAACACCTG-3′, DR53: 5′-TGAATTCCACAGTCACTTGGCTTC-3′, and DR2 probe: 5′-GACACGTGATACAAAGCCCAGGGAA-3′. For immunoglobulin D-J_H and V-DJ_H rearrangements (26): 5′D: 5′-GTCAAGGGATCTACTACTGTG-3′, V7183: 5′-GAGAGAATTCAGAGACAATCCCAAGAACACCCTG-3′, VJ558L: 5′-GAGAGAATTCTCCTCCAGCACAGCCTACATG-3′, J2: 5′-GAGAGAATTCGGCTCCCAATGACCCTTTCTG-3′, 5′ intervening sequence (IVS): 5′-GTAAGAATGGCCTCTCCAGGT-3′, 3′-IVS: 5′-GACTCAATCACTAAGACAGCT-3′, and probe: a 6-kb EcoRI fragment covering the J region of mouse IgM.

Cell Survival Determination. 8–10-wk-old *Ku70*$^{-/-}$ and *Ku80*$^{-/-}$ mice and wild-type littermates were used for our studies. Bone marrow cell suspensions were prepared by flushing the femur with MEM supplemented with 15% FCS. The cell suspension was then

counted using a hemacytometer and centrifuged at 1,000 rpm for 12 min. The resulting pellet was resuspended and diluted to $\sim 10^6$ cells/ml in MEM plus 15% FCS for further experiments.

To measure the survival of granulocyte–macrophage progenitors, the method of Van Zant et al. (29) was used with minor modifications (30). In brief, α-MEM contained 30% heat-inactivated FCS and 1% bovine serum albumin; in addition, 0.5 ng/ml GM-CSF (R & D Sys. Inc., Minneapolis, MN) was used as a source of colony-stimulating factor. 1 d before each experiment, 2.0 ml of the above media containing 0.5% noble agar (Difco Labs., Detroit, MI) was added to individual 60-mm petri dishes. Immediately after radiation exposure, cells were diluted in 2 ml of the above media with 0.3% noble agar and poured over the prepared dishes with 0.5% noble agar underlayer. The cells were then incubated at 37°C with 5% CO_2 and 95–98% humidity. The colonies were counted on day 8 with a dissecting microscope. Macrophage and granulocyte colonies were counted separately and then summed together for survival calculations of granulocyte–macrophage progenitors (granulocyte/macrophage CFUs, CFU-GM). Only colonies containing ⩾50 cells were scored. The colony forming efficiency of CFU-GMs was 60–100/10^5 nucleated cells for untreated controls. Surviving fraction was defined as the cloning efficiency of irradiated marrow cells relative to that of untreated controls. All experiments were performed at least twice and yielded consistent results.

Asymmetric Field Inversion Gel Electrophoresis. To determine the rate and extent of DNA DSB repair in Ku-deficient cells after exposure to ionizing radiation, primary embryo fibroblasts derived from *Ku70*$^{-/-}$, *Ku80*$^{-/-}$ and wild-type littermate mice were used. Mouse embryo fibroblasts from day 13.5 embryos growing in replicate cultures for 3 d in the presence of 0.01 μCi/ml [^{14}C]thymidine (New England Nuclear, Boston, MA) and 2.5 μM cold thymidine were exposed to 40 Gray (Gy) of x-rays and returned to 37°C. At various times thereafter, one dish was removed and trypsinized on ice; single cell suspensions were made and embedded in an agarose plug at a final concentration of 3×10^6 cells/ml. Asymmetric field inversion gel electrophoresis (AFIGE) was carried out in 0.5% Seakem agarose (FMC Bioproducts, Rockland, ME; cast in the presence of 0.5 μg/ml ethidium bromide) in 0.5 × TBE (45 mM Tris, pH 8.2, 45 mM boric acid, 1 mM EDTA) at 10°C for 40 h by applying cycles of 1.25 V/cm for 900 s in the direction of DNA migration, and 5.0 V/cm for 75 s in the reverse direction as described (31).

Quantification and analysis for DNA DSB present were carried out in a PhosphorImager (Molecular Dynamics, Sunnyvale, CA). Levels of DNA DSB were quantified by calculating the fraction of activity released from the well into the lane in irradiated and unirradiated samples, which equals the ratio of the radioactivity signal in the lane versus that of the entire sample (well plus lane).

Results

Targeted Disruption of Ku70 Gene. To study the role of Ku70 in vivo, we generated mice containing a germline disruption of the *Ku70* gene. Murine genomic *Ku70* gene was isolated and a targeting vector was constructed (Fig. 1 *A*). Homologous replacement results in a deletion of 336-bp exon 2, including the translational initiation codon. Two targeted ES clones carrying the mutation in *Ku70* were injected into C57BL/6 blastocysts to generate chimeric mice. One clone was successfully transmitted through the germline after chimeras were crossed with C57BL/6 females. No obvious defects were observed in *Ku70*$^{+/-}$ heterozygotes, and these *Ku70*$^{+/-}$ mice were subsequently used to generate *Ku70*$^{-/-}$ mice (Fig. 1 *B*). 25% of the offspring born from *Ku70*$^{+/-}$ × *Ku70*$^{+/-}$ crosses were *Ku70*$^{-/-}$. Adult *Ku70*$^{-/-}$ mice are fertile, but give reduced litter size (two to four pups) as compared to the *Ku70*$^{+/-}$ or *Ku70*$^{+/+}$ mice (about eight pups).

To confirm that the disruption produced a null mutation, Ku70 protein expression was analyzed by both Western blotting (Fig. 1 *C*) and a DNA end binding assay (Fig. 1 *D*). Ku70 immunoreactivity was undetectable (Fig. 1 *C*), and there was no Ku–DNA-end–binding activity in *Ku70*$^{-/-}$ fibroblasts (Fig. 1 *D*). The Ku80 subunit of the Ku heterodimer was found, but at much reduced levels (Fig. 1 *C*), suggesting that the stability of Ku80 is compromised by the absence of Ku70. These observations are consistent with the finding that the level of Ku70 was significantly reduced in *Ku80*$^{-/-}$ fibroblasts and *Ku80*$^{-/-}$ ES cells (19). Taken together, these data suggest that the stability of either component of Ku is compromised by the absence of the other.

Newborn *Ku70*$^{-/-}$ mice were 40–60% smaller than their *Ku70*$^{+/-}$ and *Ku70*$^{+/+}$ littermates. During a 5-mo observation period, *Ku70*$^{-/-}$ mice grew and maintained body weight at 40–60% of controls. Thus, *Ku70*$^{-/-}$ mice, like *Ku80*$^{-/-}$ mice, are proportional dwarfs (19).

Development of B Lymphocytes, but Not T Lymphocytes, Is Blocked at Early Stage in Ku70$^{-/-}$ *Mice.* Examination of vari-

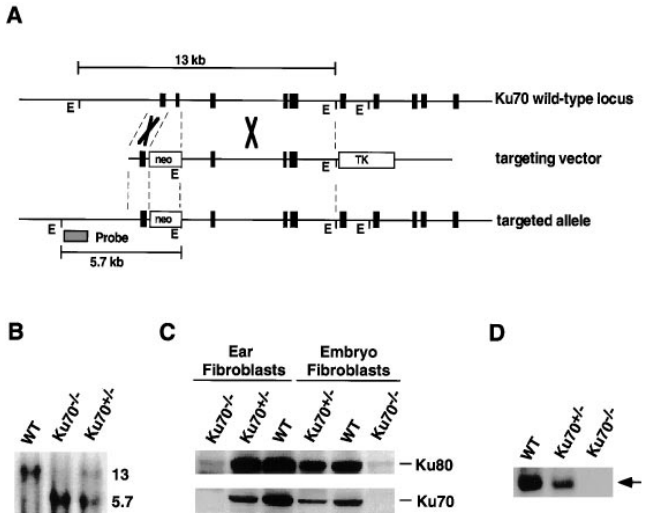

Figure. 1. Inactivation of *Ku70* by homologous recombination. (*A*) Diagrammatic representation of the *Ku70* locus (*top*), the targeting construct (*middle*), and the targeted allele and hybridization probe (*bottom*). EcoRI (*E*) restriction sites used to detect the targeted gene are indicated (21). (*B*) Southern blot of EcoRI-digested tail DNA from control wild-type (*WT*), heterozygous (+/−), and homozygous (−/−) *Ku70*-targeted mice. The wild-type and mutant fragments are 13 and 5.7 kb, respectively. (*C*) Western blot analysis showing that Ku70 protein is not expressed in *Ku70*$^{-/-}$ cells. Whole cell lysates prepared from mouse ear fibroblasts (50 μg) and mouse embryo fibroblasts (100 μg) were separated by 10% SDS-PAGE, transferred to a nitrocellulose membrane, and probed with polyclonal antibodies against full-length rodent Ku80 (*top*) and Ku70 (*bottom*), respectively. (*D*) Gel mobility shift assay (22) showing the lack of DNA-end–binding activity in *Ku70*$^{-/-}$ cells. Ku-DNA–binding complex is indicated by arrow on the right.

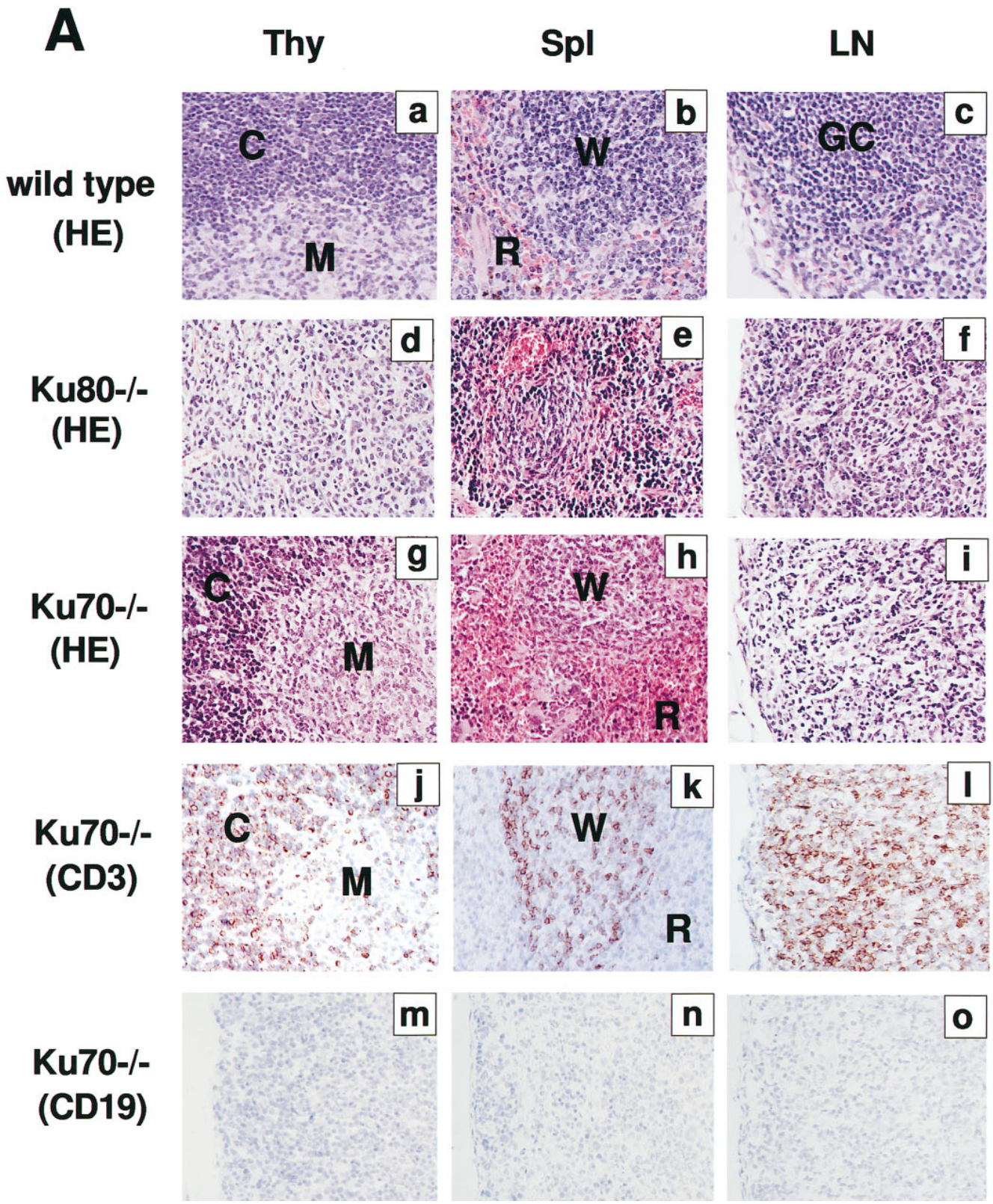

Figure 2.

ous organs from *Ku70*$^{-/-}$ mice showed abnormalities only in the lymphoid system (Fig. 2 *A*). Spleen and lymph nodes were disproportionately smaller by 5–10-fold relative to controls. In particular, splenic white pulp nodules were significantly reduced. Immunohistochemistry on deparaffinized tissue sections revealed that the splenic white pulp contained cells that stained with anti-CD3 (i.e., CD3-positive T cells), but there were no CD19-positive B cells (Fig. 2 *A*, *k* and *n*).

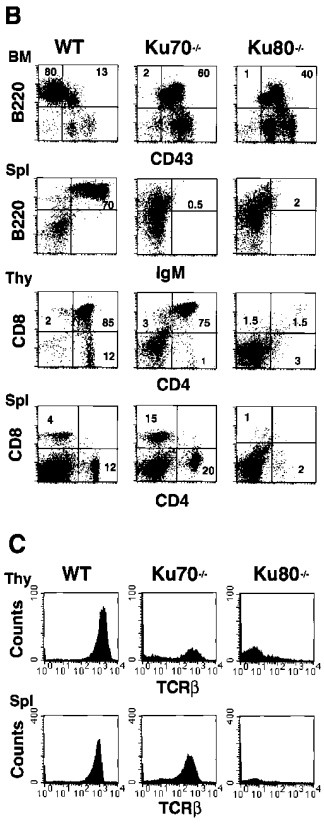

Figure 2. Development of B lymphocytes, but not T lymphocytes, is blocked at an early stage in *Ku70*$^{-/-}$ mice. (*A*) Histology of thymus (*Thy*), lymph nodes (*LN*) and spleens (*Spl*) from wild-type control mice, *Ku70*$^{-/-}$ mice, and *Ku80*$^{-/-}$ mice (23). Cortex (*C*) and medulla (*M*) are indicated. *W*, white pulp; *R*, red pulp; *GC*, germinal center. (*a–i*) Tissue sections were stained with haematoxylin and eosin (*HE*); (*j–l*) tissue sections were stained with anti-CD3 (*CD3*); and (*m–o*) tissues were stained with anti-CD19 (*CD19*). Anti-CD3 and anti-CD19 antibodies were tested in both frozen and paraffin sections of wild-type lymphoid organs and showed the expected specific patterns of staining (data not shown). (*B*) Flow cytometric analysis of thymocytes (*Thy*) bone marrow (*BM*) and spleen (*Spl*) cells from *Ku70*$^{-/-}$ mice, *Ku70*$^{+/+}$ littermates, and *Ku80*$^{-/-}$ mice. *CD4*, anti-CD4 monoclonal antibody; *CD8*, anti-CD8 monoclonal antibody; *B220*, anti-B220 monoclonal antibody; *CD43*, anti-CD43 monoclonal antibody; *IgM*, anti-Igμ heavy chain monoclonal antibody. The data were gated for live lymphoid cells based on forward and side scatter properties; 10,000–20,000 cells were analyzed per sample. (*C*) Analysis of TCR-β chain expression in *Ku70*$^{-/-}$ mice. Thymocytes and spleen cells were obtained from *Ku70*$^{-/-}$, *Ku80*$^{-/-}$, and wild-type littermates and analyzed for expression of CD4, CD8, and TCR-β by three-color flow cytometry. The TCR-β expression of both CD4$^+$ and CD8$^+$ SP T cells were shown.

The *Ku70*$^{-/-}$ thymus was also disproportionately smaller and contained 50–100-fold fewer lymphocytes than *Ku70*$^{+/+}$ littermates (3×10^6 in the former versus 2×10^8 in the latter; measured in three mice of each genotype). In contrast to the *Ku80*$^{-/-}$ mice, the *Ku70*$^{-/-}$ thymus displayed normal appearing cortical-medullary junctions (Fig. 2 *A*, *g* and *j*). Overall, the lymphoid tissues and organs of *Ku70*$^{-/-}$ mice are somewhat disorganized and much smaller than *Ku70*$^{+/+}$ mice (Table 1); yet, they are relatively more developed and slightly larger than in *Ku80*$^{-/-}$ mice.

To further examine the immunological defect in *Ku70*$^{-/-}$ mice, cells from thymus, bone marrow, and spleen were analyzed using monoclonal antibodies specific for lymphocyte surface markers and flow cytometry (19). Consistent with the immunohistological data, there was a complete block in B cell development at the B220$^+$CD43$^+$ stage in the bone marrow, and there were no mature B cells in the spleen (Fig. 2 *B*). In contrast, thymocytes developed through the CD4$^+$CD8$^+$ double-positive stage and matured into CD4$^+$CD8$^-$ and CD4$^-$CD8$^+$ single-positive (SP), TCR-β–positive cells (Fig. 2, *B* and *C*). In six 4-wk-old Ku70$^{-/-}$ mice analyzed, the percentage of CD4$^-$CD8$^-$ double-negative thymocytes ranged from 11 to 62%, and the CD4$^+$CD8$^+$ double-positive cells varied from 35 to 73%. CD4$^-$CD8$^+$ (1–11%) and CD4$^+$CD8$^-$ (1–3%) SP cells were also detected in the thymus. Furthermore, CD4$^+$CD8$^-$ or CD4$^-$CD8$^+$ SP T cells were found in the spleen in 67% of the mice studied (Fig. 2 *B*), which expressed surface TCR-β (Fig. 2 *C*) and CD3 (data not shown). Thus, in contrast to the early arrest of both T and B cell development in *Ku80*$^{-/-}$ mice (Fig. 2 *B*), lack of Ku70 is compatible with the maturation of T cells.

Table 1. *Lymphoid Cellularity of Ku70*$^{-/-}$ *Mice*

Tissue and genotype	Cell content (x 10^6)		
	Total	B220$^+$	CD4$^+$CD8$^+$
Thymus			
wild type ($n = 4$)	155 ± 42	–	104 ± 28
Ku70$^{-/-}$ ($n = 3$)	2.98 ± 0.91	–	0.6 ± 0.2
Ku80$^{-/-}$ ($n = 2$)	1.0 ± 0.5	–	–
Bone marrow			
wild type ($n = 4$)	11.9 ± 3.3	5.5 ± 1.5	–
Ku70$^{-/-}$ ($n = 3$)	7.2 ± 2.9	1.1 ± 0.4	–
Ku80$^{-/-}$ ($n = 2$)	9.0 ± 3.0	–	–
Spleen			
wild type ($n = 4$)	53 ± 20	29 ± 11	–
Ku70$^{-/-}$ ($n = 3$)	6.5 ± 1.3	0.4 ± 0.2	–
Ku80$^{-/-}$ ($n = 2$)	1.2 ± 0.5	–	–

Data shown are arithmetic means ± standard deviations from two to four individuals of each genotype analyzed at 4–6 wk of age. Cell numbers are shown per femur for bone marrow, and per whole organ for spleen and thymus.

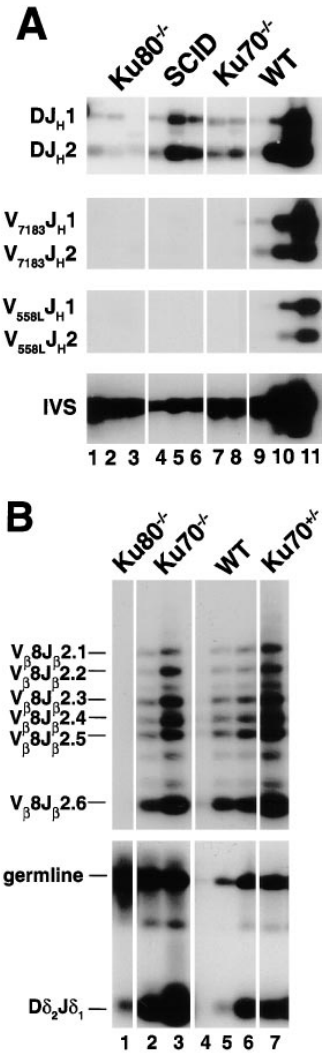

Figure 3. TCR and immunoglobulin gene rearrangement in *Ku70*$^{-/-}$ mice. (*A*) Recombination of V558L, V7183 to DJ_H, and D_H to J_H gene segments (26). 100 ng DNA was used for *Ku70*$^{-/-}$ (lanes *7* and *8*), *Ku80*$^{-/-}$ (lanes *1–3*), and *scid* mice (lanes *4–6*), and 1, 10, and 100 ng for wild-type (WT) mice (lanes *9–11*). For IVS controls, DNA was diluted 100-fold before PCR. (*B*) PCR analysis of TCR gene rearrangements. Thymus DNA was assayed for recombination of $V_\beta 8$-$J_\beta 2$ and Dδ2 to Jδ1 rearrangements (20, 27, 28). 100 ng DNA was used for *Ku70*$^{-/-}$ (lanes *2* and *7*), *Ku80*$^{-/-}$ (lane *1*), and *Ku70*$^{+/-}$ mice (lane *7*), and 1, 10, and 100 ng for wild-type mice (lanes *4–6*). Controls include a 1-kb germline interval amplified in the Dδ2 to Jδ1 intervening region (germline), and a nonrecombining segment of the Ig locus between J_H and C_H1 (not shown). The same thymus DNA samples were examined for $V_\beta 8$-$J_\beta 2$ and Dδ2 to Jδ1 recombination. Abbreviations: DJ_H, D_H to J_H rearrangements; $V_{7183}J_H$ and $V_{558L}J_H$, V7183 and V558L to DJ_H rearrangements (26); $V_\beta 8J_\beta 2.1$ to $V_\beta 8J_\beta 2.6$, $V_\beta 8$ to $DJ_\beta 2$ rearrangements (28); *germline*, unrecombined DNA from the Dδ2 to Jδ1 interval; $D\delta_2J\delta_1$, Dδ2 to Jδ1 rearrangements (20, 27); IVS, nonrecombining segment of the Ig locus between J_H and C_H1 (26). Multiple lanes underneath each genotype label (*Ku70*$^{-/-}$, *Ku80*$^{-/-}$, and *SCID*) represent different individual animals.

T-Cell Receptor and Immunoglobulin Gene Rearrangement. To determine whether a null mutation in Ku70 affects antigen-receptor gene recombination, DNA from bone marrow was amplified with primers specific to immunoglobulin D-J_H and V-DJ_H rearrangements and DNA from thymus was amplified with primers that detected V-DJ_β and D_δ-J_δ rearrangements (20, 25–28). Fig. 3 *A* shows that *Ku70*$^{-/-}$ B cells do undergo D-J_H recombination at a level which is similar to *Ku80*$^{-/-}$ B cells, but is 2–3-fold lower than the level found in *scid* mice, and 10–50-fold lower than wild-type littermates. It is possible that some, but not all, of the decrease in D-J_H rearrangement is due to a lower fraction of B lineage cells in the mutant sample, since the wild-type littermate mice have only approximately 5-fold more $B220^+$ cells than the *Ku70*$^{-/-}$ mice (see Table 1). V-DJ_H rearrangements were not detected in either *Ku70*$^{-/-}$, *Ku80*$^{-/-}$, or *scid* bone marrow samples, possibly accounting for the absence of mature B cells in these mutant mice (Fig. 3 *A*).

In contrast to the immunoglobulin heavy chain gene recombination, semiquantitative PCR analysis of thymocyte DNA for V-DJ_β joints showed normal levels of TCR-β rearrangements on a per cell basis (Fig. 3 *B*). Similarly, $D_\delta 2$ and $J_\delta 1$ coding joints were found in *Ku70*$^{-/-}$ thymocytes at levels that resembled the wild type. To determine the molecular nature of the amplified coding joints, cloned $V_\beta 8$-$DJ_\beta 2.6$ joints were sequenced. We found normal numbers of N and P nucleotides, as well as normal levels of coding end deletions (Fig. 4). Thus, coding joints in *Ku70*$^{-/-}$ thymocytes differ from coding joints produced in xrs6 Ku80-deficient cells in that there were no large aberrant deletions (4, 18). We conclude that TCR V(D)J recombination in vivo does not require Ku70.

Absence of Ku70 Confers Radiation Hypersensitivity and Deficiency in DNA DSB Repair. To assess radiation sensitivity in the absence of Ku70, cells from the bone marrow were exposed to ionizing radiation and were assayed for colony formation (30, 32). Fig. 5 *A* shows the survival curves of the CFU-GM from *Ku70*$^{-/-}$, *Ku80*$^{-/-}$, and wild-type control mice. CFU-GM from Ku70-deficient mice were more sensitive to ionizing radiation than those from Ku-proficient control mice (Fig. 5 *A*). Similar hypersensitivity to radiation was seen for Ku80$^{-/-}$ CFU-GM (Fig. 5 *A*).

The rate and extent of rejoining of x-ray–induced DNA DSB in *Ku70*$^{-/-}$, *Ku80*$^{-/-}$, and *Ku70*$^{+/+}$ cells were measured using AFIGE (31). Fibroblasts derived from day 13.5 embryos were exposed to 40 Gy of x-rays and returned to 37°C for repair. At various times thereafter, cells were prepared for AFIGE to quantitate DNA DSB (Fig. 5 *B*, *top*). DNA DSB were nearly completely rejoined in wild-type cells within ~2 h after radiation exposure. However, fibroblasts derived from *Ku70*$^{-/-}$ mice showed a drastically reduced ability to rejoin DNA DSB. A similar deficiency in DNA DSB rejoining was also observed in fibroblasts derived from *Ku80*$^{-/-}$ embryos. Despite the large differences observed in rejoining of DNA DSB between wild-type fibroblasts and fibroblasts derived from *Ku70*$^{-/-}$ or *Ku80*$^{-/-}$ mouse embryos, dose-response experiments showed that *Ku70*$^{-/-}$, *Ku80*$^{-/-}$, and wild-type fibroblasts were equally susceptible to x-ray–induced damage (Fig. 5 *B*, *bottom*). Thus, Ku deficiency primarily affects the ability of cells to rejoin radiation-induced DNA DSB without significantly affecting the induction of DNA damage.

Discussion

Absence of Ku70 results in radiation hypersensitivity and proportional dwarfism, as well as deficiencies in DNA DSB repair and V(D)J recombination. Thus, *Ku70*$^{-/-}$ mice resemble *Ku80*$^{-/-}$ mice in several respects, but the two mutations differ in their effects on T and B cell development. Lack of Ku70 was compatible with TCR gene rearrangement and development of mature $CD4^+CD8^-$ and $CD4^-CD8^+$ T cells, whereas mature T cells were absent in *Ku80*$^{-/-}$ mice. In contrast, B cells failed to complete anti-

V_β8.1	P	N	D_β2.1	N	P	J_β2.6
AGCTGTATATTTCTGTGCCAGCAGTGATG			**GGGACTGGGGGGGC**			**CTCCTATGAACAGTACTTCGGTCCCGGCACCA**
AGCTGTATATTTCTGTGCCAGCAGTG			GGAC	AGT		TGAACAGTACTTCGGTCCCGGCACCA(2)
AGCTGTATATTTCTGTGCCAGC			GG			CTCCTATGAACAGTACTTCGGTCCCGGCACCA
AGCTGTATATTTCTGTGCCAGC		CGACA	GGGGGG			CTATGAACAGTACTTCGGTCCCGGCACCA
AGCTGTATATTTCTGTGCCAGCAGTGA		CTG	GGGA			GAACAGTACTTCGGTCCCGGCACCA
V_β8.2						
ATCAGTGTACTTCTGTGCCAGCGGTGATG						
ATCAGTGTACTTCTGTGCCAGCGGTG			GGGGGGGC	TT		TGAACAGTACTTCGGTCCCGGCACCA
ATCAGTGTACTTCTGTGCCAGCGG			G			GAACAGTACTTCGGTCCCGGCACCA
ATCAGTGTACTTCTGTGCCAGCGGTA		GCC				GTACTTCGGTCACGGCTCCA
ATCAGTGTACTTCTGTGCCAGC			GG	T	AG	CTCCTATGAACAGTACTTCGGTCCCGGCACCA
ATCAGTGTATTTCTGTGCCAGC			GG			TGAACAGTACTTCGGTCCCGGCACCA
ATCAGTGTACTTCTGTGCCAGCGGTGA		CA	GGGA			CTCCTATGAACAGTACTTCGGTCCCGGCACCA
V_β8.3						
ATCTTTGTACTTCTGTGCCAGCAGTGATG						
ATCTTTGTACTTCTGTGCCAGCAGTGATG	CA		GGGG			CCTATGAACAGTACTTCGGTCCCGGCACCA
ATCTTTGTACTTCTGTGCCAGC			TG			TACTTCGGTCCCGGCACCA
ATCTTTGTACTTCTGTGCCAGCAGTGAT			C			CCTATGAACAGTACTTCGGTCCCGGCACCA
ATCTTTGTACTTCTGTGCCAGCAGTGAT			TGGG			CCTATGAACAGTACTTCGGTCCCGGCACCA
ATCTTTGTACTTCTGTGCCAGCAGTGA						CCTATGAACAGTACTTCGGTCCCGGCACCA

Figure 4. Nucleotide sequences of $V_\beta8D_\beta2.1J_\beta2.6$ junctions from the thymus of a 4-wk-old *Ku70*$^{-/-}$ mouse. Products corresponding to Vβ8.1, Vβ8.2, or Vβ8.3 rearrangement with $J_\beta2.6$ were cloned and sequenced. TCR $V_\beta8$-$J_\beta2$ joints were amplified by PCR (20, 27, 28) as described (see Fig. 3 *B*). PCR cycling conditions were 94°C for 45 s, 58°C for 30 s, and 72°C for 30 h (30 cycles). The band corresponding to $V_\beta8$-$J_\beta2.6$ was purified, reamplified for 20 cycles, and then subcloned into the pCRII vector (Invitrogen, San Diego, CA). DNA was extracted from individual colonies and sequenced using the universal T7 and M13 reverse primers. Germline sequences are written in boldface; *N* and *P*, nucleotides not present in the germline sequences.

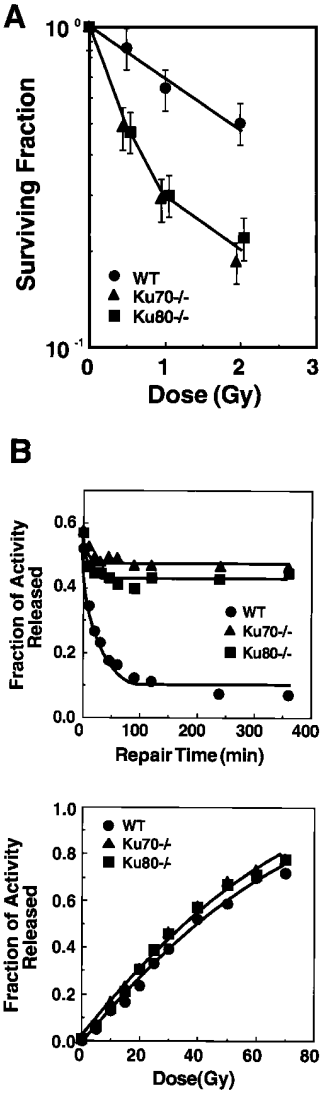

Figure 5. Disruption of Ku70 confers radiation hypersensitivity and a deficiency in DNA DSB repair. (*A*) Radiation survival curves for the CFU-GM in the bone marrow of wild type (*WT*), *Ku70*$^{-/-}$, and *Ku80*$^{-/-}$ mice (30, 32). (*B*) Deficiency in the repair of radiation-induced DSB in *Ku70*$^{-/-}$ and *Ku80*$^{-/-}$ cells (31). (*Top*) Rejoining of DNA DSB produced by 40 Gy x-ray. (*Bottom*) Induction of DNA DSB as a function of the radiation dose in wild-type, *Ku70*$^{-/-}$, and *Ku80*$^{-/-}$ cells. ●, wild type; ▲, *Ku70*$^{-/-}$; and ■, *Ku80*$^{-/-}$ cells, respectively.

gen receptor gene rearrangement and did not mature in either *Ku70*$^{-/-}$ or *Ku80*$^{-/-}$ mice.

What could account for the differences we find in TCR and immunoglobulin gene rearrangements in the *Ku70*$^{-/-}$ mice? One implication of our findings is that there are alternative Ku70-independent rescue pathways that are compatible with completion of V(D)J recombination in T cells. It is likely at the critical phase of T cell maturation, other DNA repair activity may be stimulated (33, 34) and can functionally complement the Ku70 gene in T cell–specific V(D)J recombination. Since *Ku80*$^{-/-}$ mice are deficient in both T and B lymphocyte development, it is plausible that these yet to be identified alternative DNA repair pathways include Ku80. The much reduced level of Ku80 protein in *Ku70*$^{-/-}$ cells may in part account for the hypocellularity of *Ku70*$^{-/-}$ thymuses.

Although the role of Ku in V(D)J recombination is not molecularly defined, Ku has been proposed to protect DNA ends from degradation (18, 35), to activate DNA-PK (10, 11), and to dissociate the recombination-activating protein RAG–DNA complex to facilitate the joining reaction (20). These functions are not mutually exclusive, and they are all dependent on the interaction of Ku with DNA. Thus, the finding that Ku70 is not required for TCR gene rearrangement is particularly unexpected because the Ku70 subunit is believed to be the DNA-binding subunit of the Ku complex (36), and DNA-end–binding activity was not detected in Ku70-deficient cells (Fig. 1 *D*).

In summary, our studies provide direct evidence supporting the involvement of Ku70 in the repair of DNA DSB and V(D)J recombination and the presence of a Ku70-independent rescue pathway(s) in TCR V(D)J rearrangement. The distinct phenotype of *Ku70*$^{-/-}$ mice should make them valuable tools for unraveling the mechanism(s) of DNA repair and recombination.

We thank D. Roth for PCR primers, D. Kim and L. Wu for Ku antiserum, T. Deloherey for FACS® analysis, P. Krechmer for word processing, A. Haimovitz-Friedman and Hatsumi Nagasawa for valuable suggestions, and C.C. Ling and Z. Fuks for advice and support.

The work was supported in part by National Institutes of Health grants CA-31397 and CA-56909 (to G.C. Li), CA-42026 (to G. Iliakis), CA-50519 (to D.J. Chen), and Department of Energy Office of Health and Environmental Research (to D.J. Chen). A. Nussenzweig is a research fellow supported by National Institutes of Health training grant CA61801 and M. Nussenzweig is an associate investigator in the Howard Hughes Medical Institute.

Address correspondence to G.C. Li, Department of Medical Physics and Department of Radiation Oncology, Memorial Sloan-Kettering Cancer Center, 1275 York Ave./Box 72, New York, NY 10021. Phone: 212-639-6028; FAX: 212-639-2611; E-mail: g-li@ ski.mskcc.org

Received for publication 23 May 1997 and in revised form 14 July 1997.

References

1. Li, Z., T. Otevrel, Y. Gao, H.-L. Cheng, B. Sneed, T. Stamato, G. Taccioli, and F.W. Alt. 1995. The *XRCC4* gene encodes a novel protein involved in DNA double-strand break repair and V(D)J recombination. *Cell*. 83:1079–1089.
2. Hendrickson, E.A., X.-Q. Qin, E.A. Bump, D.G. Schatz, M. Oettinger, and D.T. Weaver. 1991. A link between double-strand break-related repair and V(D)J recombination: the *scid* mutation. *Proc. Natl. Acad. Sci. USA*. 88:4061–4065.
3. Pergola, F., M.Z. Zdzienicka, and M.R. Lieber. 1993. V(D)J recombination in mammalian cell mutants defective in DNA double-strand break repair. *Mol. Cell. Biol*. 13:3464–3471.
4. Taccioli, G.E., G. Rathbun, E. Oltz, T. Stamato, P.A. Jeggo, and F.W. Alt. 1993. Impairment of V(D)J recombination in double-strand break repair mutants. *Science (Wash. DC)*. 260: 207–210.
5. Roth, D.B., T. Lindahl, and M. Gellert. 1995. How to make ends meet. *Curr. Biol*. 5:496–499.
6. Bogue, M., and D.B. Roth. 1996. Mechanism of V(D)J recombination. *Curr. Opin. Immunology*. 8:175–180.
7. Jeggo, P.A., G.A. Taccioli, and S.P. Jackson. 1995. Menage a trois: double strand break repair, V(D)J recombination and DNA-PK. *Bioessays*. 17:949–956.
8. Weaver, D.T. 1995. What to do at an end: DNA double-strand-break repair. *TIG (Trends Genet.)* 11:388–392.
9. Biedermann, K.A., J. Sun, A.J. Giaccia, L.M. Tosto, and J.M. Brown. 1991. *scid* mutation in mice confers hypersensitivity to ionizing radiation and a deficiency in DNA double-strand break repair. *Proc. Natl. Acad. Sci. USA*. 88:1394–1397.
10. Dvir, A., S.R. Peterson, M.W. Knuth, H. Lu, and W.S. Dynan. 1992. Ku autoantigen is the regulatory component of a template-associated protein kinase that phosphorylates RNA polymerase II. *Proc. Natl. Acad. Sci. USA*. 89:11920–11924.
11. Gottlieb, T.M., and S.P. Jackson. 1993. The DNA-dependent protein kinase: requirement for DNA ends and association with Ku antigen. *Cell*. 72:131–142.
12. Lees-Miller, S.P. 1996. The DNA-dependent protein kinase, DNA-PK: 10 years and no ends in sight. *Biochem. Cell Biol*. 74:503–512.
13. Peterson, S.R., A. Kurimasa, M. Oshimura, W.S. Dynan, E.M. Bradbury, and D.J. Chen. 1995. Loss of the catalytic subunit of the DNA-dependent protein kinase in DNA double-strand-break-repair mutant mammalian cells. *Proc. Natl. Acad. Sci. USA*. 92:3171–3174.
14. Kirchgessner, C.U., C.K. Patil, J.W. Evans, C.A. Cuomo, L.M. Fried, T. Carter, M.A. Oettinger, and J.M. Brown. 1995. DNA-dependent kinase (p350) as a candidate gene for the murine SCID defect. *Science (Wash. DC)*. 267:1178–1183.
15. Blunt, T., N.J. Finnie, G.E. Taccioli, G.C.M. Smith, J. Demengeot, T.M. Gottlieb, R. Mizuta, A.J. Varghese, F.W. Alt, P.A. Jeggo, and S.P. Jackson. 1995. Defective DNA-dependent protein kinase activity is linked to V(D)J recombination and DNA repair defects associated with the murine scid mutation. *Cell*. 80:813–823.
16. Boubnov, N.V., K.T. Hall, Z. Wills, S.E. Lee, D.M. He, D.M. Benjamin, C.R. Pulaski, H. Band, W. Reeves, E.A. Hendrickson, and D.T. Weaver. 1995. Complementation of the ionizing radiation sensitivity, DNA end binding, and V(D)J recombination defects of double-strand break repair mutants by the p86 Ku autoantigen. *Proc. Natl. Acad. Sci. USA*. 92:890–894.
17. Smider, V., W.K. Rathmell, M.R. Lieber, and G. Chu. 1994. Restoration of x-ray resistance and V(D)J recombination in mutant cells by Ku cDNA. *Science (Wash. DC)*. 266: 288–291.
18. Taccioli, G.E., T.M. Gottlieb, T. Blunt, A. Priestly, J. Demengeot, R. Mizuta, A.R. Lehmann, F.A. Alt, S.P. Jackson, and P.A. Jeggo. 1994. Ku80: product of the *XRCC5* gene and its role in DNA repair and V(D)J recombination. *Science (Wash. DC)*. 265:1442–1445.
19. Nussenzweig, A., C. Chen, V. da Costa Soares, M. Sanchez, K. Sokol, M.C. Nussenzweig, and G.C. Li. 1996. Requirement for Ku80 in growth and immunoglobulin V(D)J recombination. *Nature (Lond.)*. 382:551–555.
20. Zhu, C., M.A. Bogue, D.-S. Lim, P. Hasty, and D.B. Roth. 1996. Ku86-deficient mice exhibit severe combined immunodeficiency and defective processing of V(D)J recombination intermediates. *Cell*. 86:379–389.
21. Takiguchi, Y., A. Kurimasa, F. Chen, P.E. Pardington, T. Kuriyama, R.T. Okinaka, R. Moyzis, and D.J. Chen. 1996. Genomic structure and chromosomal assignment of the mouse Ku70 gene. *Genomics*. 35:129–135.
22. Kim, D., H. Ouyang, S.-H. Yang, A. Nussenzweig, P. Burgman, and G.C. Li. 1995. A constitutive heat shock element–binding factor is immunologically identical to the Ku-autoantigen. *J. Biol. Chem*. 270: 15277–15284.
23. Serrano, M., H.-W. Lee, L. Chin, C. Cordon-Cardo, D. Beach, and R.A. DePinho. 1996. Role of the *INK4a* in tu-

mor suppression and cell mortality. *Cell*. 85:27–37.
24. Cordon-Cardo, C., and V.M. Richon. 1994. Expression of the retinoblastoma protein is regulated in normal human tissue. *Am. J. Pathol*. 144:500–510.
25. Ausubel, F.M., R. Brent, R.E. Kingston, D.D. Moore, J.G. Seidman, J.A. Smith, and K. Struhl. 1997. Current Protocols in Molecular Biology. John Wiley & Sons, New York.
26. Costa, T.E.F., H. Suh, and M. Nussenzweig. 1992. Chromosomal position of rearranging gene segments influences allelic exclusion in transgenic mice. *Proc. Natl. Acad. Sci. USA*. 89: 2205–2208.
27. Roth, D.B., C. Zhu, and M. Gellert. 1993. Characterization of broken DNA molecules associated with V(D)J recombination. *Proc. Natl. Acad. Sci. USA*. 90:10788–10792.
28. Bogue, M.A., C. Zhu, E. Aguilar-Cordova, L.A. Donehower, and D.B. Roth. 1996. p53 is required for both radiation-induced differentiation and rescue of V(D)J rearrangement in scid mouse thymocytes. *Genes Dev*. 10:553–565.
29. Van Zant, G., D. Flentje, and M. Flentje. 1983. The effect of hyperthermia on hemopoietic progenitor cells of the mouse. *Radiat. Res*. 95:142–149.
30. Mivechi, N.F., and G.C. Li. 1985. Thermotolerance and profile of protein synthesis in murine bone marrow cells after heat shock. *Cancer Res*. 45:3843–3849.
31. Illiakis, G., L. Metzger, N. Denko, and T.D. Stamato. 1991. Detection of DNA double-strand breaks in synchronous cultures of CHO cells by means of asymmetric field inversion gel electrophoresis. *Int. J. Radiat. Biol*. 59:321–341.
32. Fulop, G.M., and R.A. Phillips. 1990. The *scid* mutation in mice causes a general defect in DNA repair. *Nature (Lond.)*. 347:479–482.
33. Strasser, A., A.W. Harris, L.M. Corcoran, and S. Cory. 1994. Bcl-2 expression promotes B- but not T-lymphoid development in *scid* mice. *Nature (Lond.)*. 368:457–460.
34. Danska, J.S., F. Pflumio, C.J. Williams, O. Huner, J.E. Dick, and C.J. Guidos. 1994. Rescue of T cell–specific V(D)J recombination in SCID mice by DNA-damaging agents. *Science (Wash. DC)*. 266:450–455.
35. Liang, F., and M. Jasin. 1996. Ku80-deficient cells exhibit excess degradation of extrachromosomal DNA. *J. Biol. Chem*. 271:14405–14411.
36. Chou, C.H., J. Wang, M.W. Knuth, and W.H. Reeves. 1992. Role of a major autoepitope in forming the DNA binding site of the p70 (Ku) antigen. *J. Exp. Med*. 175:1677–1684.